POD analysis of flame dynamics from optical imaging of an IC Engine

Katarzyna Bizon[1], Gaetano Continillo[2], Simona S. Merola[3] and Bianca Maria Vaglieco[3]

[1]Istituto Ricerche Combustione CNR, Via Diocleziano 328, 80124 Naples, Italy
[2]Universita del Sannio, Department of Engineering, Piazza Roma 1, 82100 Benevento, Italy
[3]Istituto Motori CNR, Via Marconi, 80125 Naples, Italy

1. Introduction

Even though relatively high acquisition frequencies are nowadays attained for high resolution images of the combustion chamber, analysis of morphological and geometrical properties of the flame requires high time resolution. Particularly, available techniques provide high space resolution images – but collected over different cycles. Cycle-to-cycle variations and thermal drift are two of the main problems in collecting and using such data to study time evolution of the flame. In fact, whilst frame averaging over different test sessions can be used to compensate for cycle–to–cycle variations at the price of information loss, each test session cannot last too long due to experimental engine overheating and this limits the number of values of the crank angle that can be collected in each test session and, as a consequence, the – even simulated – time sampling rate cannot be so high as it would be desirable. In earlier works, various interpolation or reconstruction techniques have been proposed and applied to ICE imaging experimental data [1,2]. Generally, reconstruction techniques based on physical concepts have proved to work better as compared to pure mathematical interpolation [3]. In this work, flame images are collected and recorded and then Proper Orthogonal Decomposition (POD) [4] coupled with interpolation is applied to reconstruct information in between consecutive measurements. More precisely, POD basis is determined from samples taken during experiments conducted on an optically accessible Internal Combustion Spark Ignition Engine [5]. Each experimental data set contains a number N of successive frames (512x512 pixels) collected during a number of cycles at varying crank angle. First, POD is applied to space and time resolved experimental data of flame luminosity taken over a number of cycles and varying crank angles in order to determine empirical eigenfunctions, which describe the dominant behavior of the system. Next, POD coefficients are calculated by performing the orthogonal projection of the ensemble of data onto the set of eigenfunctions. The coefficients are interpolated over the crank-angle in order to reconstruct the luminosity field between consecutive measurements. Reconstructed luminosity fields are then compared with the available (but not used in the computations) experimental data.

2. Experimental

Figure 1 shows the experimental apparatus for spectroscopic, 2D-digital imaging and chemiluminescence measurements, along with a schematic diagram and a photograph of the engine used in the present investigation. This is an optically accessible single cylinder ported fuel injection (PFI) spark ignition (SI) engine. The piston is flat and made transparent through a quartz window (Φ=57mm). The optical path includes an inclined (45°) mirror located in the bottom of the engine. The engine has a specially machined cylinder head of a four valve commercial automotive engine with a pent–roof combustion chamber and the spark plug was centrally located. During combustion, the light emitted through the quartz window is reflected towards the optical detection assembly by a 45° inclined UV–visible mirror located at the bottom of the engine. The mirror has elliptical shape (47×66 mm): its size allows to collect images from a large portion of the chamber, as shown in Figure 2. During spectroscopic investigations the combustion light emission was focused by an UV lens (100 mm focal length) onto micrometer controlled entrance slit of a spectrometer with 150 mm focal length, f/3.8 aperture, 300 groove/mm grating (Fig. 1a). In order to investigate natural emissions from ultraviolet to visible, the central wavelength of spectrometer was fixed at 400 nm. The output of the spectrometer (250 nm spectral range) was

coupled to an intensified cooled CCD camera (ICCD) with an array size of 512x512 pixels and 16-bit dynamic range digitisation at 100 kHz. The ICCD spectral range spread from UV (180 nm) until visible (700 nm).
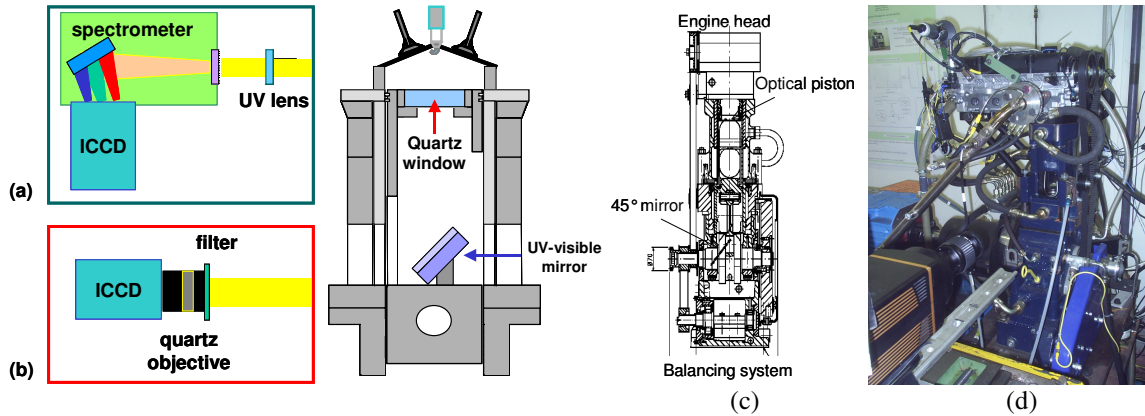

Figure 1. Schematic diagrams of experimental apparatus for (a) spectroscopic, (b) digital imaging and chemiluminescence measurements. To the right, drawing and photograph of the PFI SI engine.
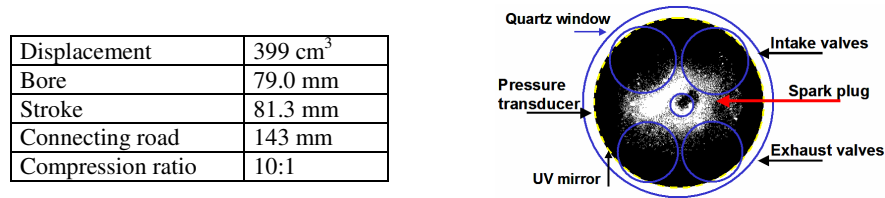
Displacement	399 cm^3
Bore	79.0 mm
Stroke	81.3 mm
Connecting road	143 mm
Compression ratio	10:1

Figure 2. To the left: engine specifications; to the right: Field of view of the combustion chamber.

The ICCD can acquire high space resolution images but not more than one per cycle. This results in CAD sequences that do not belong to the same cycle. There are three ways to construct a time-resolved sequence: Single shot (one per crank angle), short exposure time, one test session (high spatial definition ↔ uncorrelated time sequence); Single shot (one per crank angle), long exposure time, one test session (lower spatial definition ↔ more regular flame pattern); *N* accumulated shots per crank angle, multiple test sessions (blurred spatial definition ↔ more correlated averaged time sequence).

2. POD Method

Suppose we are given a time series, obtained from simulation or experiment, $u_t(x)$ where *t* denotes time and *x* denotes position in space. In practice, in numerical models the spatial domain is discretised and the number of time samples is finite, therefore usually the sampled data set is a vector–valued function given as a matrix:

$$U = \begin{bmatrix} u_1(x_1) & u_2(x_1) & \cdots & u_M(x_1) \\ u_1(x_2) & u_2(x_2) & \cdots & u_M(x_2) \\ \vdots & \vdots & \ddots & \vdots \\ u_1(x_N) & u_2(x_N) & \cdots & u_M(x_N) \end{bmatrix}$$

where *N* is the number of positions in the spatial domain and *M* is the number of samples taken in time. It can be shown that a suitable POD basis $\Phi = \{\varphi_1, \varphi_2, \ldots, \varphi_N\}$ is obtained by solving the eigenvalue problem $C\Phi = \lambda\Phi$ where *C* is the averaged autocorrelation matrix $C(x, x') = \langle U(x), U(x') \rangle$ and brackets denote time-averaging. Using the POD modes, the solution $u_t(x)$ can be expressed by a linear combination of the eigenfunctions:

$$\tilde{u}_k(x) = \sum_{k=1}^{K} a_k(t) \varphi_k(x) \qquad (1)$$

where $K < N$ is the number of modes used for truncation and a_k are modal coefficients that can be determined by projection of the ensemble of data onto the POD modes. In this work we use the Sirovich approach (see Holmes

et al. 1996). Namely, when – as in this case – the number of collected time samples is smaller than the space discretization, it is more efficient to assume that the eigenfunctions are linear combinations of the snapshots:

$$\varphi(x) = \sum_{i=1}^{M} b_i u_i(x)$$

Hence, substituting into the original POD problem we obtain $CB = \lambda B$, where C is the space correlation matrix:

$$C_{ij} = \frac{1}{N} \sum_{k=1}^{N} u_i(x_k) u_j(x_k)$$.

The POD eigenvalue problem is solved and the POD eigenfunctions are determined as a combination of eigenvectors and the "snapshots". The coefficients of POD eigenfunctions are calculated by conducting the orthogonal projection of the data onto the set of POD basis functions. The luminosity field is reconstructed by using different numbers K of POD eigenfunctions as per Eq. (1). The luminosity fields between successive experimental measurements (and before the first and after the last CAD) were reconstructed by performing interpolation (extrapolation) of modal coefficients a_k that are simply function of the crank angle degree.

3. Results

In this paper, the POD procedure was applied to two experimental data sets: Set 1 has 6 frames containing accumulated luminosity collected during 10 experiments for a number of cycles at varying CAD in the range of 1÷6, ΔCAD=1; Set 2 has a long sequence of single–shot successive frames collected during a number of cycles at varying CAD in the range of 0÷26.2, with ΔCAD=0.4.

In both cases the correlation matrix was calculated and the eigenvalue problem was solved in order to determine empirical eigenfunctions, which describe the dominant behavior of the system. Then, the POD coefficients, that are the function of the crank angle degree, were calculated by performing the orthogonal projection of the ensemble of data onto the set of eigenfunctions. The coefficients were interpolated over the CAD domain and the luminosity field between consecutive measurements was reconstructed. For the first data set, all six experimental accumulated luminosity snapshots were included in the computations: then 60 consecutive snapshots were reconstructed in the CAD range 0.6÷6.5, ΔCAD=0.1. In the second case, since we had long time series, the procedure was checked against experimental data. Only snapshots with odd indexes were used to determine the basis: hence, we were able to compare the reconstructed luminosity fields with the available, but not used in the computations, experimental data.

Set 1. The leading "eigenflame" for this data set captures in more than 96% of the correlation energy, hence it should be able to describe correctly the dominant behavior of the luminosity field. Figure 3 compares the sequence of the six experimental frames (on top) and the corresponding reconstruction with one eigenflame (dominant POD mode, bottom). On the right, the reconstruction error is displayed.
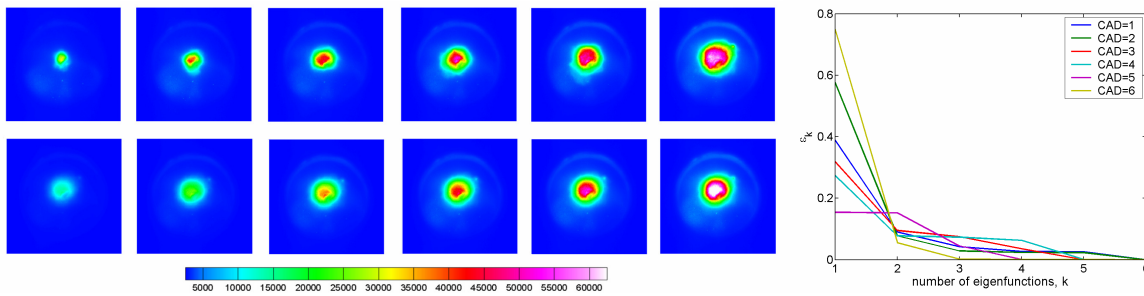

Figure 3. Sequence of the six experimental frames (on top) and the corresponding reconstruction with one eigenflame (dominant POD mode, bottom) for CAD between 1 and 6. On the right, reconstruction error.

We define the relative average error of the k_{th} order POD reconstruction as:

$$\varepsilon_k = \frac{1}{N_x N_y u_{avg}^2} \sum_{i=1}^{N_x} \sum_{j=1}^{N_y} \left[u(x_{ij}) - \tilde{u}_k(x_{ij}) \right]^2, \quad \text{where} \quad u_{avg} = \frac{1}{N N_x N_y} \sum_{k=1}^{N} \sum_{i=1}^{N_x} \sum_{j=1}^{N_y} u(x_{ijk}).$$

As expected, the relative error decreases with increasing the number of eigenfunctions employed. A dependence of the error on the crank angle also exists, although non monotonic. Interpolation was then used to construct

frames in between experimental images. Figure 4 shows such an "artificial" sequence from, obtained with POD/Spline interpolation by using all of six eigenmodes.
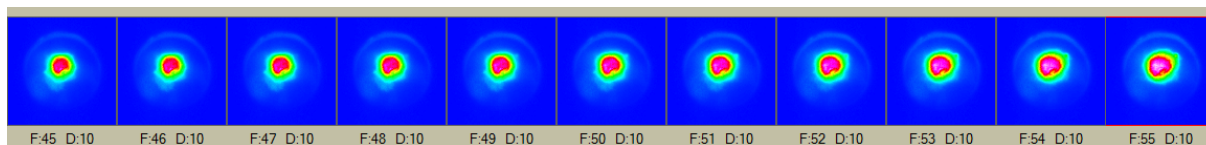
Figure 4. POD/Spline reconstructed frames between experimental at CAD=5 (F:45) and CAD=6 (F:55).

Set 2. The single-shot experimental sequence delivers a much clearer definition but has an irregular character, due to the fact that shots cannot be acquired in the same engine cycle. Both features are clearly seen in Figure 5, top row. The bottom row shows the "artificial" sequence produced by using all 32 modes extracted by applying POD analysis to the odd-numbered experimental frames. Odd frames are coincident with experimental whereas the "artificial" even-numbered frames are rather different from the available experimental shots taken at corresponding crank angles. The POD/Linear interpolation delivers, as expected, a more regular time sequence.
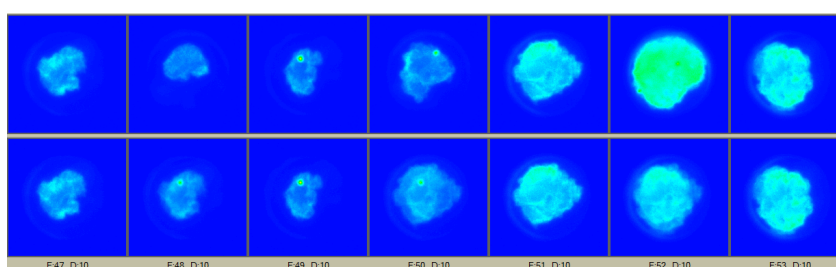
Figure 5. Experimental (top) and POD/Linear reconstructed sequence of single-shot images.

4. Conclusions

Results of reconstruction from POD basis proved to be successful when checked against available experiments even with just one basis function. The single–shot time sequence from experiments suffers from being uncorrelated, nevertheless the basis set built from one half of available shots permits a veritable reconstruction of intermediate frames not included in the decomposition. Future work will address the construction of POD basis from repeated single–shot frames individually considered rather than accumulated. Also, reconstruction of sequences from frames taken at different crank angle but in one cycle (even with less resolution) will be attempted.

References

1. M. Fogelman, J. Lumley, D. Rempfer, D. Haworth (2004), Application of the proper orthogonal decomposition to datasets of internal combustion engine flows, J. of Turbulence 5 023 (http://jot.iop.org/)
2. P. Druault, P. Guibert and F. Alizon (2005), Use of proper orthogonal decomposition for time interpolation from PIV: Application to the cycle-to-cycle variation analysis of in-cylinder engine flows, Experiments in Fluids 39, 1009-1023
3. H. Gunes, S. Sirisup and G.E. Karniadakis (2006), Gappy data: To Krig or not to Krig? Journal of Computational Physics 212, 358-382
4. P. Holmes, J.L. Lumley, G. Berkooz, 1996, "Turbulence, Coherent Structures, Dynamical Systems and Symmetry", Cambridge University Press, p.86
5. S.S. Merola and B.M. Vaglieco, Knock investigation by flame and radical species detection in spark ignition engine for different fuels, Proc. ECOS2006 Conference, paper n°230
6. Sirovich, L. (1987). Turbulence and the Dynamics of Coherent Structures, Quarterly of Applied Mathematics, 45, 561–590